IEEE Access
Multidisciplinary | Rapid Review | Open Access Journal

Received February 8, 2021, accepted February 15, 2021, date of publication February 16, 2021, date of current version March 2, 2021.

*Digital Object Identifier 10.1109/ACCESS.2021.3059926*

# Toward an Electroactive Polymer-Based Soft Microgripper

**CHIA-JU PENG[1,4], LAURÉLINE SEURRE[2], ÉRIC CATTAN[2], GIAO TRAN-MINH NGUYEN[3], CÉDRIC PLESSE[3], LUC CHASSAGNE[1], (Member, IEEE), AND BARTHÉLEMY CAGNEAU[1]**

[1]LISV, Université de Versailles Paris-Saclay (UVSQ), 78140 Vélizy, France
[2]CNRS, Université de Lille, Yncréa, Centrale Lille, UMR 8520-IEMN, DOAE, Université Polytechnique Hauts-de-France, 59300 Valenciennes, France
[3]LPPI, CY Cergy Paris Université, F-95000 Cergy, France
[4]Department of Mechanical Engineering, National Central University, Taoyuan 320317, Taiwan

Corresponding author: Barthélemy Cagneau (barthelemy.cagneau@uvsq.fr)

This work was supported in part by the French National Research Agency (ANR) through the Project MicroTIP under Grant ANR-15-CE08-0032.

**ABSTRACT** Grasping and manipulating objects on a microscale hold great promise, especially using mechanical structures made from soft materials that enable, for example, safe operations during micro-surgery. Soft robots should be preferred to manipulate micro-objects, but their adoption requires, inter alia, soft transducers that can operate either in air or in solution. Ultimately, they should enable actuation at low voltage, as well as be easy to fabricate. This paper presents the results on our investigations about conducting polymers-based transducers. We demonstrate that this material is suitable to construct sensitive structures and a microgripper is proposed to illustrate the results. Large strains were observed and a grasping force of 0.17 mN was generated. Moreover, compared to previous work, we show that the fabrication process can be downscaled while preserving the behavior of the material in both actuation and sensing modes. The macroscale mechanical models obtained are still valid for microscale actuation and sensing.

**INDEX TERMS** Electroactive polymers, microgripper, smart materials.

## I. INTRODUCTION

A microgripper is one of the key elements in microrobotics technology for handling objects in very confined spaces without causing any damage. The essential components of all microgrippers are the actuating and sensing parts required to interact with objects and control the gripper in space. The structure should be able to accurately control the position of small, delicate objects and, at the same time, should be monitored to avoid excessive forces being exerted between the structure and the objects. Consequently, several challenges need to be addressed to propose an efficient reliable microgripper: a large force-to-weight ratio, quasi-static motions to enable high resolution positioning, a large stroke to interact with objects of different shapes, and force feedback capability to monitor the interactions.

Various actuation methods and microstructure types for microgrippers have been considered in the literature: piezoelectric grippers [1]–[4] produce small displacements and forces despite being actuated with high voltages. Thermally driven grippers with piezoresistors [5], [6] produce locally high temperatures. In contrast to the above solutions, electrostatically driven comb actuators exhibit high displacement capabilities but generate low amplitude forces [7]–[10]. In [11]–[14], shape-memory alloy-based grippers are interesting solutions but their sensitivity to the temperature makes them unsuitable for certain applications.

Moreover, the rigidity of the previous structures may lead to stiff interactions with the objects manipulated and are difficult to integrate beside or inside structures in soft microrobotics. To overcome this difficulty and to produce higher displacements, several investigations have been carried out on polymer materials. Some are very convenient to actuate, sense, or even both [15]. Among them, pneumatically-driven microgrippers [16]–[18] do not have an embedded actuation mechanism, which prevents miniaturization. Thermally activated polymers, including some hydrogels [19]–[23], are sensitive to ambient and body temperature. However, in both cases, they do not include sensing functions. For polymeric microgrippers, great efforts have been made in the last ten years to reduce the high electrical voltages required to drive dielectric polymers [24]. Finally, the use of external laser sources is problematic for liquid-crystalline networks [25],

The associate editor coordinating the review of this manuscript and approving it for publication was Michail Kiziroglou.

[26] and some hydrogels [23] when microgrippers must be inserted inside living tissue.

Ionic electroactive polymer micro-arms such as ionic polymer-metal composites and conducting polymer-based actuators are promising and enable the manipulation of small objects in air or aqueous solution. They are actuated at low voltages, typically under $2.0V$, consequently preventing electrolysis while actuating in water. Additionally, these materials are suitable to operate as sensors. For this class of materials, electronic conducting polymer (ECP) based trilayer structures consist of a central membrane sandwiched between two layers of the conducting polymer. The central membrane acts as an ionic reservoir used to operate the device. For thin films ($< 30\mu m$), when a low voltage ($< 2.0V$) is applied, the ECP is oxidized or reduced electrochemically. Ions and solvent molecules are then inserted or expelled through the membrane to ensure overall electroneutrality, resulting in a variation in the ECP volume and a bending motion. Conversely, when a mechanical stimulation is applied to the trilayer, a voltage can be measured. Besides these characteristics, ECP-based trilayer structures are lightweight, noiseless, biocompatible, downsizable and can present large strains. These structures are, therefore, promising candidates for fabricating microgrippers with electronic conducting polymers.

In [27], initial results have demonstrated the ability to use these materials as grippers to control the pressure applied to an object. However, these materials were manufactured traditionally and remain massive and bulky. To overcome this shortcoming, studies have been conducted to reduce the thicknesses and the lateral dimensions of these transducers [28] to move toward microgrippers with a volume of interest that is less than a cubic millimeter. The scale effects will therefore have an impact on the mechanical characteristics and on the sensitivity to detect the strain. Consequently, the changes in the design process may affect the results obtained previously in [27].

In section II, we describe the different steps necessary to design the material. Next, in section III, we recall the main equations obtained to control the structure on a macroscale [27]. Experiments were carried out to evaluate the performance of the material and to validate the models suitable to control it in an open loop. A microgripper is then presented in section IV to demonstrate the dual functionalities of the material for both sensing and actuation while lifting a small object. Finally, a brief comparison between the materials designed on a macro- and microscale is proposed in the conclusion.

## II. FABRICATION PROCESS

Compared to the material we used in previous work [27], the fabrication process has been modified to miniaturize the transducer. First, we have changed to microfabrication technologies. Next, the conductive polymer has been changed from poly(3,4-ethylenedioxythiophene) (PEDOT) to poly(3,4-ethylenedioxythiophene):poly(styrene sulfonate) (PEDOT:PSS). PEDOT requires a washing step to remove the oxidant and any residual EDOT when synthesizing, whereas PEDOT:PSS does not require a washing step. Moreover, PEDOT:PSS has the advantage of being easy to process by using drop-casting, spray coating, and spin coating [29].

The fabrication process of the micro-transducer based on sequential layer stacking is shown in Figure 1. The PEDOT:PSS electrodes with PEO network precursors were fabricated using the casting method. The procedures of the process are as follows [28]:

1) Preparation of the first electrode: the formulated PEDOT:PSS casting solution is prepared by mixing 40wt% of PEO precursors with respect to the solid content of Clevios PH1000 commercial solution. The PEO precursors are composed of 50wt% poly ethylene glycol methyl ether methacrylate (PEGM), 50wt% polyethyleneglycol dimethacrylate (PEGDM), and ammonium persulfate (APS, 3wt% with respect to the total mass of PEGM and PEGDM). The PEDOT:PSS solution is retrieved using a micropipette ($0.08\ mL.cm^{-2}$) and deposited within a delimited area inside a mold to guarantee that the same surface is cast. Before water evaporation, it is checked that the solution is homogeneously distributed to obtain a constant thickness.
2) The substrate is placed on a hot plate at $50°\ C$ to evaporate the water and form the electrode.
3) Preparation of the ion reservoir membrane: Nitrile Butadiene Rubber (NBR) is dissolved in cyclohexanone (20wt%) and stirred until complete dissolution. 50wt% PEO network precursors with respect to NBR content are added to the reaction mixture (PEO precursors composed of 50/50 wt% PEGM and PEGDM). 3wt% (with respect to PEO precursor) of dicyclohexyl peroxidicarbonate (DCPD), as a free radical initiator of PEO precursor polymerization, is finally added to the reaction mixture. The PEO/NBR reaction mixture is spin coated onto the first PEDOT:PSS/PEO electrode layer.
4) Pre-polymerization in a sealed chamber under argon for 45 min at $50°\ C$ to initiate the formation of the PEO network.
5) The second PEDOT:PSS/PEO electrode layer is fabricated on top of the PEO/NBR layer in the same way as step 1.
6) The substrate is placed on a hot plate at $50°\ C$ to evaporate the water and solidify the second electrode.
7) The substrate is placed in a sealed chamber under argon for the final heat treatment for 3h at $50°\ C$ and 1h at $80°\ C$ to achieve the free radical polymerization of the PEO precursors within the PEDOT:PSS/PEO electrodes, the PEO/NBR ionic conducting membrane, and at their interface.
8) The fabrication process of the tri-layer is completed.
9) The trilayer structures are patterned to define the micro-transducers using laser cutting.
10) Lift off and immersion of the microtransducers in ionic liquid (1-ethyl-3-methylimidazolium

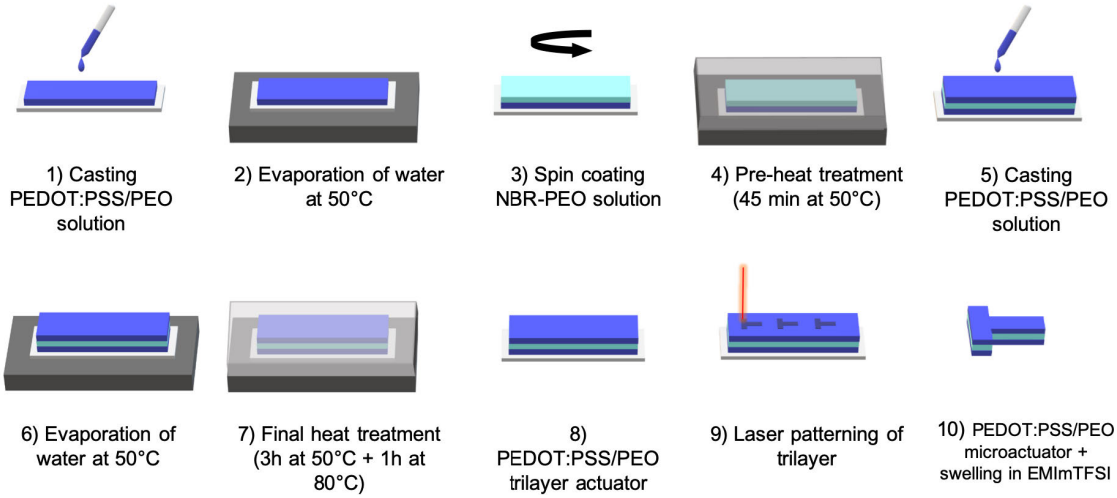


**FIGURE 1.** Layer-by-layer synthesis of the micro-transducer.

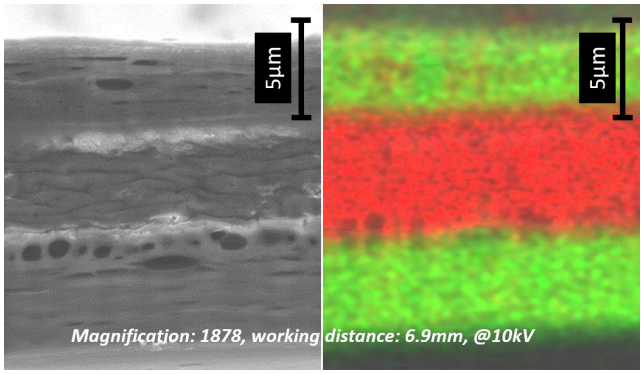


**FIGURE 2.** Left: SEM image of the cross-section of a PEDOT:PSS/POE-NBR/POE-PEDOT:PSS/POE micro-beam. Right: PEDOT:PSS/PEO is characterized by the presence of sulfur (in green on the image) allowing this layer to be distinguished from that of NBR-POE identifiable by the absence of sulfur.

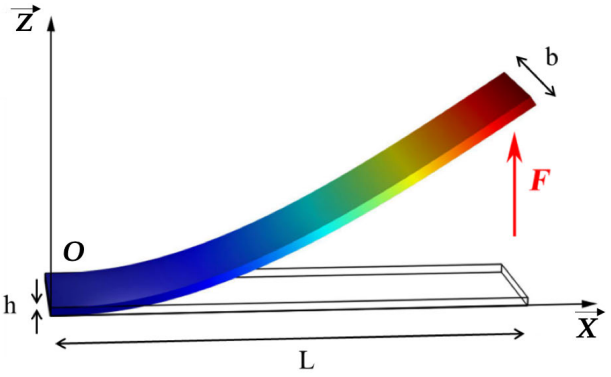


**FIGURE 3.** Mechanical model of the cantilever. As an actuator, the force $F$ generated deforms the polymer itself and can be used for grasping. Conversely, as a sensor, the external force $F$ applied to the tip can be approximately obtained with the corresponding deformation.

bis(trifluoromethanesulfonyl)imide, 72h) to incorporate the ions necessary for the redox process.

Figure 2 shows the scanning electron microscope (SEM) energy-dispersive X-ray spectroscopy (EDX) images of the cross-section of a final microtransducer. The PEDOT:PSS/PEO layers are discernable by the sulfur element (green), which is not present in the central NBR/PEO layer, characterized by the carbon element (red).

Thereafter, we will be interested in microactuators and microsensors configured as cantilevers connected to a circuit board. The dimensions are 4.2 $mm \times 1.2\ mm \times 29.6\mu m$. Young's modulus of the trilayer structure was 0.9 $GPa$ [28]. In the next section, models and experiments are provided in both actuation and sensing modes. Ultimately, these results will be compared to those obtained on a macroscale and presented in [30].

## III. PERFORMANCES OF THE TRANSDUCERS

### A. MECHANICAL MODELING

The mechanical model has been described previously in [27]. In the following paragraphs, we recall the main results to provide the reader with an overview of the models and to improve understanding of the experiments conducted in the following sections. We would like to determine if the previous models are still valid with the new downscaled fabrication process. Due to the scope of soft microrobotics, it would also be useful to stick with the models that do not require advanced techniques for identification.

The system used to model the mechanical deformations is presented in Figure 3.

The length, width, and thickness of the cantilever are noted $L$, $b$, and $h$ , respectively. As described in [31], we defined the dimensionless coordinates $(x, z)$, in the $(O, \vec{X}, \vec{Z})$ frame, as functions of a dimensionless abscissa.

Let us define the dimensionless length $l$ as:

$$l = s_f - s_i \tag{1}$$

where $s_f$ is the curvilinear abscissa of the tip of the rod and $s_i$ relates to the other extremity.

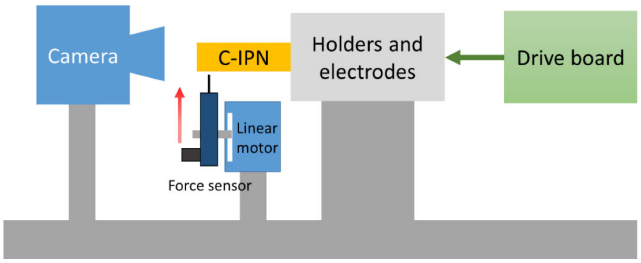


**FIGURE 4.** Experimental setup to measure the output voltage of the polymer transducer and to track its motions.

The dimensioned coordinates of the rod are given by:

$$\begin{cases} X(S) = -\dfrac{L}{l}\left[x\left(\dfrac{l}{L}S + s_i\right) - x(s_i)\right] \\ Z(S) = \dfrac{L}{l}\left[z\left(\dfrac{l}{L}S + s_i\right) - z(s_i)\right] \end{cases} \tag{2}$$

where $S \in [0, L]$ denotes the dimensioned curvilinear abscissa.

The coordinates defined in equation 2 are used to model the shape of the polymer with respect to the time. Based on this measurement, they allow the computation of the force applied by the actuator. Its value $F$ is computed according to equation 3:

$$F = EI \cdot \left(\frac{l}{L}\right)^2 \tag{3}$$

where $E$ and $I$ are the Young's modulus and the moment of inertia of the sample, respectively.

### B. EXPERIMENTAL SETUP

The experimental setup is presented in Figure 4 and is dedicated to the measurement of the displacements and forces modeled in section III-A.

A camera was attached to the system to record the motions of the polymer transducers. While actuating, image processing techniques were used to capture the shape of the polymer in real-time with a spatial resolution of $17.1\mu m$. A microforce sensing probe was also used to monitor the forces. This force sensor was mounted on a linear motor that can move towards the tip of the polymer and produce a mechanical disturbance. Therefore, the probe also enabled us to characterize the polymer in sensing mode.

### C. PERFORMANCE AS ACTUATORS

#### 1) DISPLACEMENTS

For all the experiments, the dimensions of the sample were $4.2\ mm \times 1.2\ mm \times 29.6\mu m$. The input voltage was set to $2.0\ V$ and the polymer was actuated for one minute. The camera monitored the displacements of the polymer and the successive shapes are presented in Figure 5 for several time values.

We observed that the deformation angle was quite considerable as the tip of the polymer reached $Z = 3.16\ mm$ at $t = 60\ s$. The tip of the actuator moved at a speed around $0.15\ mm.s^{-1}$ in the first ten seconds. This velocity

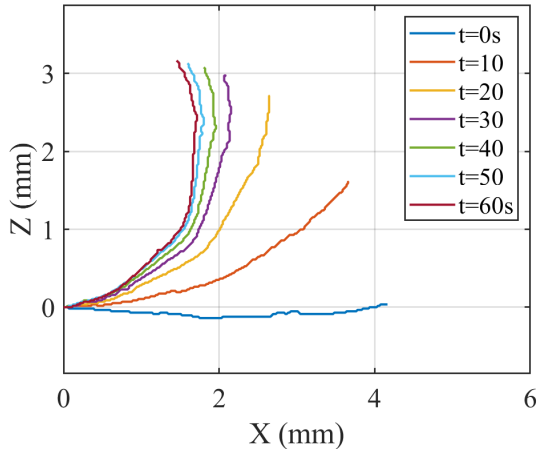


**FIGURE 5.** The curves shapes of the polymer for an actuation voltage of $2.0\ V$ at different times monitored using image tracking. The dimensions were $4.2\ mm \times 1.2\ mm \times 29.6\mu m$.

was quite low compared to other polymer actuators. However, for microgrippers and micro-robots in general, robustness and stability with respect to the input voltage should be preferred over velocity. ECP-based on trilayer structures have no back-relaxation under electrical voltage contrary to the behavior usually observed in IPMC. In addition, the materials used and the method of microfabrication of the actuators prevent any delamination between the three layers and, therefore, any premature aging of the actuator.

#### 2) BLOCKING FORCES

Here, the objective was to derive the relationship between the input voltage and the force generated by the sample to enable us to set the desired force to grasp objects, as illustrated in section IV.

In Figure 6, we were first interested in the tip displacement values with respect to the forces generated. The displacements were measured with the tracking system and the corresponding blocking forces were recorded for a given voltage. The theoretical force is computed with respect to the tip displacement (see equation 3) and compared with the experimental values. The relationship between these two values is linear as shown by equation 3.

The estimated and measured forces are plotted against the input voltage on the same figure. It can be observed that most of the results were in fair agreement with the model presented in the previous section. The maximal error was about 10% and occured when the input voltage was equal to $1.0\ V$. Regarding the experiment in section IV, this Figure is useful to predict the force generated compared to the tip displacement. We can also obtain a good estimation of the applied force with respect to the input voltage.

### D. PERFORMANCE AS SENSORS

In this section, we are interested in measurements in the sensing mode. The microforce sensing probe was driven towards the polymer with a linear stage. The applied force and the output voltage of the polymer transducer were recorded.

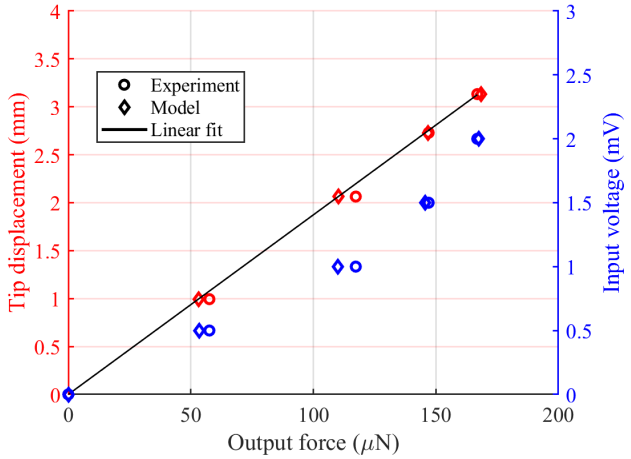


**FIGURE 6.** Driving voltage and displacement of the polymer with respect to the blocking forces.

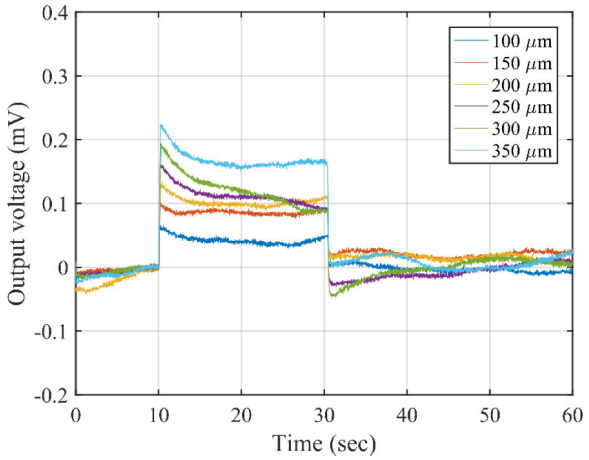


**FIGURE 7.** Output voltage of the polymer sensor with different bending displacements held for 20 sec.

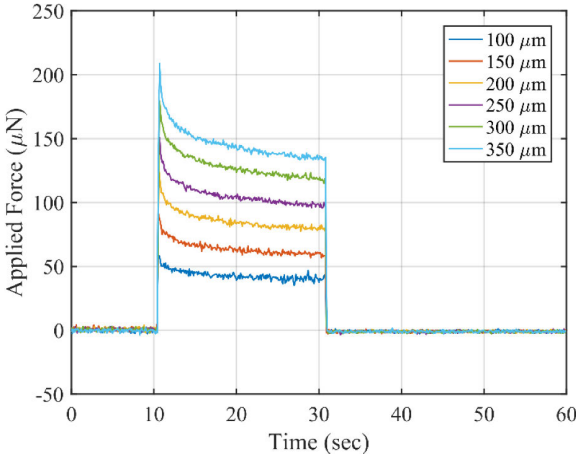


**FIGURE 8.** Bending force applied to the polymer with respect to different bending displacements. The forces values were measured with a strain detecting probe.

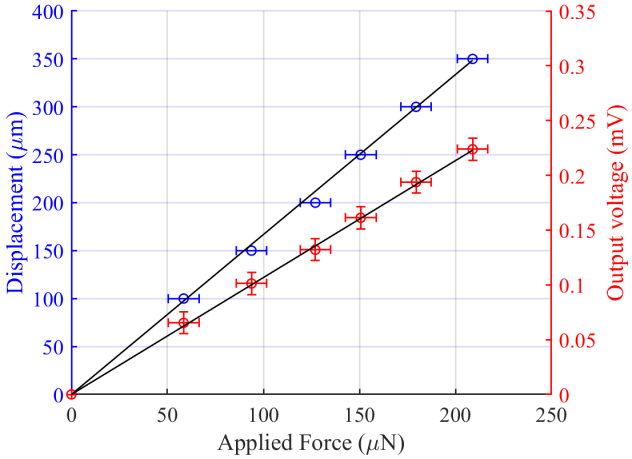


**FIGURE 9.** Displacement and output voltage of the polymer transducer with respect to the force applied.

During this experiment, the contact between the probe and the polymer occurred at $t = 10s$.

In Figure 7, the polymer was bent to varying degrees, from $100\mu m$ to $350\mu m$, and the constraint was held for 20 $s$. At the same time, the output voltage of the transducer was recorded and the results were plotted against the tip displacement.

The applied force measured with the microforce sensor is shown in Figure 8. The maximal measured forces occurred at the beginning of bending and then decayed over time while holding contact. The sensitivity of the sensing probe was high enough to detect the voltage decay over time because of the loss of induced charge.

Next, we used these values to calibrate the output voltage of the polymer transducer. The results are presented in Figure 9.

To obtain this graph, we considered the force values corresponding to the maximum output voltages measured. This choice was made to prevent excessive forces acting on the object. At the same time, it is responsible for a high uncertainty about the force set by the user. The system would benefit of an active compensation of the loss of induced charge and this solution should be investigated in a future work. The displacements are easily determined since we track the deformations in real-time with the camera. Prior to experiments, we have computed the uncertainties of the force and of the output voltage. The values of $8\mu N$ and $0.01mV$ were respectively obtained for the force and the voltage. For both computations, it was assumed that the noise obeys a Gaussian distribution.

First, we were interested in the output voltage with respect to the force. It can be observed that the relationship between the two values can be characterized as linear. The sensitivity of the polymer transducer was $0.936 \pm 0.547\ N.V^{-1}$. This value can be used to derive the forces with respect to the output voltage. In the same Figure, the displacement is plotted against the force. It also exhibits linear behavior.

## IV. DEMONSTRATION OF A POLYMER GRIPPER

### A. EXPERIMENTAL SETUP

The system comprised two similar polymer transducers measuring $4.2\ mm \times 1.2\ mm \times 29.6\mu m$. The first one, on the left, is the active finger. The second one, on the right, is the sensing part. A small piece of rubber measuring $3.5\ mm \times 2.0\ mm \times 1.5\ mm$ and with a mass of 38 $mg$ was placed between the two

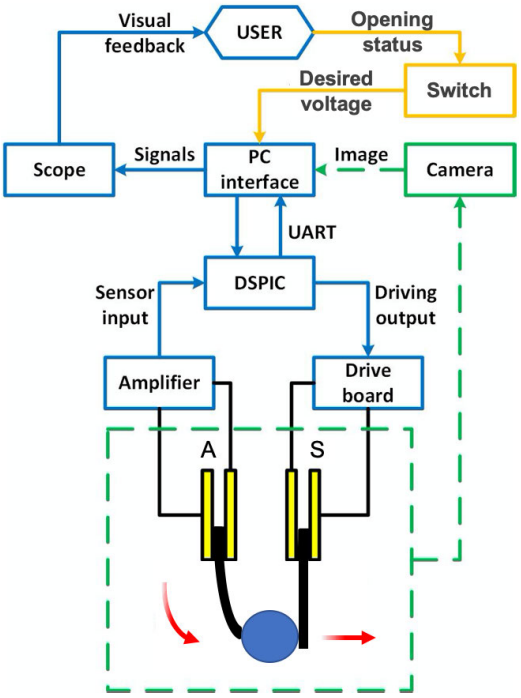


**FIGURE 10.** Overview of the architecture used to control the microgripper.

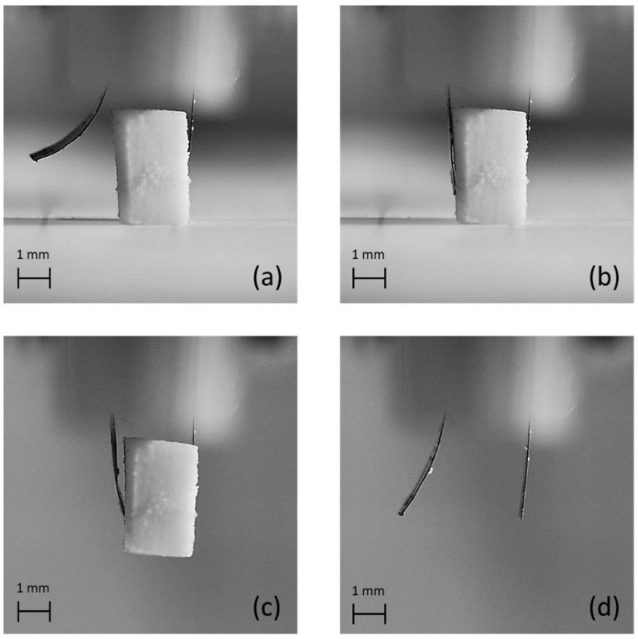


**FIGURE 11.** The grasping task consisted in (a) opening the gripper (b) closing the gripper (c) grasping and lifting an object (d) reopening the gripper and dropping the object. These pictures were extracted from the video which is available online as part of this work.

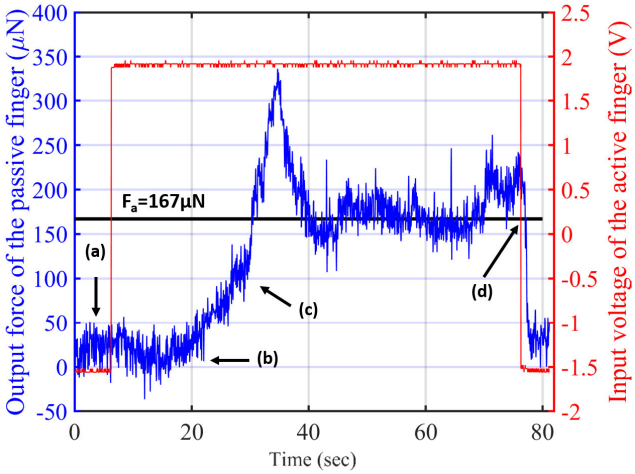


**FIGURE 12.** Measured sensing force of the passive finger (blue) and the driving voltage of the controlled active finger (red).

polymers. The two transducers were fixed to form a gripper and could be moved up and down.

Besides the gripper, an entire interface was developed to interact with the user. The different blocks are presented in Figure 10. From a hardware point of view, a home-made circuit was included with a digital to analog module (DAC) through which the signal passes to drive the active finger. A circuit was also entirely designed to amplify the output voltage of the sensing part, including a filter to remove noisy components due to the environment. The magnitude was indeed lower than a millivolt before being amplified.

Finally, the user could control the system by switching a numerical input. Depending on its status, the input voltage was set to 2.0 $V$ to close the gripper and to $-1.5V$ to open it.

### B. EXPERIMENT

In Figure 11, several steps are accomplished during the grasping experiment:

(a) First, the gripper is opened. Then, the input voltage of the active finger is switched to 2.0 $V$. The active finger begins to become into contact with the object between the fingers. According to the previous results regarding the actuating force, this input voltage corresponds to a desired force $||\mathbf{F_a}|| = 167 \pm 8\mu N$.

(b) The gripper closes and the camera tracks the displacement of the tip. The difference in potential between the two electrodes of the passive finger is measured. We can expect that the force $\mathbf{F_p}$ measured by the passive finger is such that $||\mathbf{F_p}|| \neq ||\mathbf{F_a}||$ because of the additional friction forces.

(c) The gripper is now fully closed and the object is lifted up. The active and passive fingers exert a constant force on the object once the material has reached a steady state.

(d) The input voltage of the active finger is switched back to $-1.5$ $V$ and the gripper opens. Consequently, the object is released and dropped.

The image was processed to measure the displacement of the active and passive fingers. The resolution is about 1 *pixel* $\approx 17.5\mu m$. According to the results and the models presented in sections III-C and III-D, the forces were computed and monitored in real-time while grasping.

As shown in Figure 12, the contact is established, the measured force $||\mathbf{F_p}||$ increases to reach its maximum value

| Samples properties | Macro-polymers | Micro-polymers |
|---|---|---|
| Length (mm) | 10 | 4.2 |
| Width (mm) | 4 | 1.2 |
| Thickness (μm) | 250 | 29.6 |
| Young's modulus (MPa) | 150 | 900 |
| **Actuation performances** | **Macro-polymers** | **Micro-polymers** |
| Displacement @2V (mm) | 2.41 | 3.13 |
| Blocking forces @2V (mN) | 1.92 | 0.17 |
| Slope of the force/tip displacement (N/m) | 0.81 | 0.60 |
| **Sensing performances** | **Macro-polymers** | **Micro-polymers** |
| Displacement sensitivity (V/m) | 0.14 | 0.64 |
| Force sensitivity (N/V) | 5.80 | 0.94 |

**FIGURE 13.** Comparison of macro- and micro-polymers performances.

$F_{p,max} \approx 320\mu N$ and then starts to decay. When a steady state is reached after 40 seconds, the value of $||\mathbf{F_p}||$ is around $170\mu N$. Remarkably, this value is pretty close to the value of the applied force $||\mathbf{F_a}|| = 167\mu N$. However, this result requires further analysis as we did not model the friction forces and we used the experimental values obtained in Figure 9 without actually having a physical model of the material. Finally, the signal is quite noisy because of environmental noise probably due to the driving device. When contact was broken, the measured voltage on the passive finger dropped quickly to return to its initial value.

## V. CONCLUSION

In [27], we demonstrated that polymer transducers can be used to design a gripper made of two fingers. This material demonstrates both actuation and sensing capabilities. In this paper, the fabrication process was downscaled and we were able to design a similar gripper. To compare the results between the two designs, namely macro- and micro-polymers, the main characteristics are recalled in Figure 13.

First, Young's modulus values are quite different (900 MPa $>$ 150 MPa). However, because of a lower moment of inertia, large displacements were obtained with the micro-polymer.

It has been also demonstrated that the mechanical models used for actuation are still valid when downscaling the fabrication process. This is very promising for future experiments as models enable the computation of the desired forces before driving the structure. Finally, in the near future, electroactive polymer-based transducers appear as good candidates to contribute to developments in soft microrobotics. They can operate either in air or in solution and their small dimensions are an advantage when limited workspace is an issue. The results demonstrate that the proposed methods are compatible with microfabrication technologies to reduce the size of the structures. Besides the fabrication process, the size is also reduced because the material can be used either as an actuator or a sensor to control the interactions with the manipulated objects. Another advantage of the material is its actuation with low voltages, enabling *ex vivo* and *in vivo* experiments. We believe that the gripper is the first step towards safe manipulation of fragile micro-objects. In future work, these results will be used to control the structure in a closed loop.

Moreover, a multi-finger gripper with integrated gold electrodes is currently being developed to enable complex grasping and manipulation.

## REFERENCES

[1] M. Carrozza, A. Menciassi, G. Tiezzi, and P. Dario, "The development of a LIGA-microfabricated gripper for micromanipulation tasks," *J. Micromech. Microeng.*, vol. 8, no. 2, p. 141, 1998.
[2] M. Rakotondrabe, C. Clevy, and P. Lutz, "Modelling and robust position/force control of a piezoelectric microgripper," in *Proc. IEEE Int. Conf. Autom. Sci. Eng.*, Sep. 2007, pp. 39–44.
[3] T. Abondance, K. Jayaram, N. T. Jafferis, J. Shum, and R. J. Wood, "Piezoelectric grippers for mobile micromanipulation," *IEEE Robot. Autom. Lett.*, vol. 5, no. 3, pp. 4407–4414, Jul. 2020.
[4] R. K. Jain, S. Majumder, B. Ghosh, and S. Saha, "Design and manufacturing of mobile micro manipulation system with a compliant piezoelectric actuator based micro gripper," *J. Manuf. Syst.*, vol. 35, pp. 76–91, Apr. 2015.
[5] C. G. Keller and R. T. Howe, "Hexsil tweezers for teleoperated microassembly," in *Proc. IEEE 10th Annu. Int. Workshop Micro Electro Mech. Syst. Invest. Micro Struct., Sens., Actuators, Mach. Robots*, Jan. 1997, pp. 72–77.
[6] C. S. Pan and W. Hsu, "An electro-thermally and laterally driven polysilicon microactuator," *J. Micromech. Microeng.*, vol. 7, no. 1, pp. 7–13, Mar. 1997.
[7] C.-J. Kim, A. P. Pisano, and R. S. Muller, "Silicon-processed overhanging microgripper," *J. Microelectromech. Syst.*, vol. 1, no. 1, pp. 31–36, Mar. 1992.
[8] M. Boudaoud, Y. Haddab, and Y. Le Gorrec, "Modeling and optimal force control of a nonlinear electrostatic microgripper," *IEEE/ASME Trans. Mechatronics*, vol. 18, no. 3, pp. 1130–1139, Jun. 2013.
[9] O. Millet, P. Bernardoni, S. Régnier, P. Bidaud, E. Tsitsiris, D. Collard, and L. Buchaillot, "Electrostatic actuated micro gripper using an amplification mechanism," *Sens. Actuators A, Phys.*, vol. 114, nos. 2–3, pp. 371–378, Sep. 2004.
[10] T. Chen, L. Sun, L. Chen, W. Rong, and X. Li, "A hybrid-type electrostatically driven microgripper with an integrated vacuum tool," *Sens. Actuators A, Phys.*, vol. 158, no. 2, pp. 320–327, Mar. 2010.
[11] M. Kohl, E. Just, W. Pfleging, and S. Miyazaki, "SMA microgripper with integrated antagonism," *Sens. Actuators A, Phys.*, vol. 83, nos. 1–3, pp. 208–213, May 2000.
[12] I. Roch, P. Bidaud, D. Collard, and L. Buchaillot, "Fabrication and characterization of an SU-8 gripper actuated by a shape memory alloy thin film," *J. Micromech. Microeng.*, vol. 13, no. 2, p. 330, 2003.
[13] J.-H. Lee, Y. S. Chung, and H. Rodrigue, "Long shape memory alloy tendon-based soft robotic actuators and implementation as a soft gripper," *Sci. Rep.*, vol. 9, no. 1, pp. 1–12, Dec. 2019.
[14] Y. Lu, Z. Xie, J. Wang, H. Yue, M. Wu, and Y. Liu, "A novel design of a parallel gripper actuated by a large-stroke shape memory alloy actuator," *Int. J. Mech. Sci.*, vol. 159, pp. 74–80, Aug. 2019.
[15] J. Shintake, V. Cacucciolo, D. Floreano, and H. Shea, "Soft robotic grippers," *Adv. Mater.*, vol. 30, no. 29, Jul. 2018, Art. no. 1707035.
[16] K. Suzumori, S. Iikura, and H. Tanaka, "Development of flexible microactuator and its applications to robotic mechanisms," in *Proc. IEEE Int. Conf. Robot. Automat.*, Jan. 1991, pp. 1622–1623.
[17] J. Ok, M. Chu, and C.-J. Kim, "Pneumatically driven microcage for microobjects in biological liquid," in *IEEE Int. MEMS Conf., 12th IEEE Int. Conf. Micro Electro Mech. Syst. Tech. Dig.*, Jan. 1999, pp. 459–463.
[18] J. Paek, I. Cho, and J. Kim, "Microrobotic tentacles with spiral bending capability based on shape-engineered elastomeric microtubes," *Sci. Rep.*, vol. 5, no. 1, Sep. 2015, Art. no. 10768.

[19] Z. Hu, X. Zhang, and Y. Li, "Synthesis and application of modulated polymer gels," *Science*, vol. 269, no. 5223, pp. 525–527, Jul. 1995.
[20] H.-Y. Chan and W. J. Li, "A thermally actuated polymer micro robotic gripper for manipulation of biological cells," in *Proc. IEEE Int. Conf. Robot. Automat.*, vol. 1, Sep. 2003, pp. 288–293.
[21] M. Behl, K. Kratz, J. Zotzmann, U. Nöchel, and A. Lendlein, "Reversible bidirectional shape-memory polymers," *Adv. Mater.*, vol. 25, no. 32, pp. 4466–4469, Aug. 2013.
[22] Q. Ge, A. H. Sakhaei, H. Lee, C. K. Dunn, N. X. Fang, and M. L. Dunn, "Multimaterial 4D printing with tailorable shape memory polymers," *Sci. Rep.*, vol. 6, no. 1, Nov. 2016, Art. no. 31110.
[23] C. Ma, X. Le, X. Tang, J. He, P. Xiao, J. Zheng, H. Xiao, W. Lu, J. Zhang, Y. Huang, and T. Chen, "A multiresponsive anisotropic hydrogel with macroscopic 3D complex deformations," *Adv. Funct. Mater.*, vol. 26, no. 47, pp. 8670–8676, Dec. 2016.
[24] X. Ji, A. El Haitami, F. Sorba, S. Rosset, G. T. M. Nguyen, C. Plesse, F. Vidal, H. R. Shea, and S. Cantin, "Stretchable composite monolayer electrodes for low voltage dielectric elastomer actuators," *Sens. Actuators B, Chem.*, vol. 261, pp. 135–143, May 2018.
[25] D. Martella, S. Nocentini, D. Nuzhdin, C. Parmeggiani, and D. S. Wiersma, "Photonic microhand with autonomous action," *Adv. Mater.*, vol. 29, no. 42, Nov. 2017, Art. no. 1704047.
[26] O. M. Wani, H. Zeng, P. Wasylczyk, and A. Priimagi, "Programming photoresponse in liquid crystal polymer actuators with laser projector," *Adv. Opt. Mater.*, vol. 6, no. 1, Jan. 2018, Art. no. 1700949.
[27] C.-J. Peng, O. Ameline, F. B. Ribeiro, C. Plesse, S. Haliyo, S.-J. Chen, L. Chassagne, and B. Cagneau, "Electromechanical model of a conducting polymer transducer, application to a soft gripper," *IEEE Access*, vol. 7, pp. 155209–155218, 2019.
[28] K. Rohtlaid, G. T. M. Nguyen, C. Soyer, E. Cattan, F. Vidal, and C. Plesse, "Poly(3, 4 ethylenedioxythiophene): Poly(styrene sulfonate)/polyethylene oxide electrodes with improved electrical and electrochemical properties for soft microactuators and microsensors," *Adv. Electron. Mater.*, vol. 5, no. 4, Apr. 2019, Art. no. 1800948.
[29] B. Charlot, G. Sassine, A. Garraud, B. Sorli, A. Giani, and P. Combette, "Micropatterning PEDOT: PSS layers," *Microsyst. Technol.*, vol. 19, no. 6, pp. 895–903, 2013.
[30] C.-J. Peng, F. Ribeiro, C. Plesse, S.-J. Chen, L. Chassagne, and B. Cagneau, "Electrical behavior of a self-sensing actuator made of electroactive polymers," in *Proc. 2nd IEEE Int. Conf. Soft Robot. (RoboSoft)*, Apr. 2019, pp. 212–216.
[31] A. E. H. Love, *A Treatise on the Mathematical Theory of Elasticity*. Cambridge, U.K.: Cambridge Univ. Press, 2013.

**CHIA-JU PENG** received the B.S. degree in agriculture with a minor in bio-industrial mechatronics engineering from National Taiwan University, Taipei, Taiwan, in 2012. He is currently pursuing the joint Ph.D. degree in mechanical engineering with National Center University, Taoyuan, Taiwan, and the Université de Versailles Saint-Quentin en Yvelines UVSQ / LISV, Vélizy, France. His research interests include biosignal processing, image processing, microelectromechanical systems, robotics, and transducers.

**LAURÉLINE SEURRE** received the master's degree in chemistry from the University of Cergy-Pontoise, in 2017. She is currently pursuing the Ph.D. degree in micro/nanotechnology with the Institute of Electronics, Microelectronics and Nanotechnologies (IEMN – CNRS), Université Polytechnique des Hauts-de-France (UPHF). Her research interests include electronically conducting polymers, microelectromechanical systems, and soft micro-transducer.

**ÉRIC CATTAN** received the Ph.D. degree from University Paris XI, Orsay, in 1993. In 1994, he was recruited as an Associate Professor at Laboratory of Advanced Ceramic Materials. In 2002, he joined the Institute of Electronics and Microelectronics and Nanotechnology, University of Polytechnic Hauts de France, where he became a Professor. If his career began in the field of piezoelectric and ferroelectric thin films, the last 20 years have been devoted to bioinspired MEMS. In particular, the production of a nano drone flying like an insect fabricated by using microfabrication technologies and the use of transducers, related to artificial muscles, in order to produce flexible microsystems for the medical field.

**GIAO TRAN-MINH NGUYEN** received the Ph.D. degree in chemistry and physico-chemistry of Polymer from the University of Maine, France, in 2003. From 2004 to 2005, she was with Prof. Bo Nyström's Group at University of Oslo, Norway, as a Postdoctoral Fellow, where she was working on the modification of polysaccharides. In 2008, she joined LPPI, University of Cergy Pontoise, France, as an Assistant Professor, where she was as a Postdoctoral Fellow on the synthesis of polyelectrolyte for using as Li-batteries solid electrolyte, from 2009 to 2010. Since 2010, she has been an Associate Professor. Her current research interest includes development of new electrolyte polymer system for applications in electrochemical devices such as actuators, hybrid photovoltaic systems, and Li-batteries.

**CÉDRIC PLESSE** received the Ph.D. degree in macromolecular chemistry from the University of Cergy-Pontoise, in 2004, and the HDR degree, in 2014. From 2004 to 2006, he was with Prof. Mario Leclerc's laboratory at the University of Laval, Canada, as a Postdoctoral Researcher. He was recruited as an Associate Professor with the Laboratory of Physicochemistry of Polymers and Interfaces (LPPI), University of Cergy-Pontoise, in 2006. His main research interest includes development of conducting polymer-based electrostimulable materials from the synthesis of highly conducting ionogels with interpenetrating polymer network architectures to electromechanical characterization of synthesized (macro or micro) actuators.

**LUC CHASSAGNE** (Member, IEEE) received the B.S. degree in electrical engineering from Supelec, France, in 1994, and the Ph.D. degree in optoelectronics from the University of Paris XI, Orsay, France, in 2000, for his work in the field of atomic frequency standard metrology. He is currently a Professor and the Director of the LISV laboratory, University of Versailles. His research interests include nanometrology, sensors, and visible light communications.

**BARTHÉLEMY CAGNEAU** received the Ph.D. degree from the Institute of Intelligent Systems and Robotics (ISIR), Sorbonne University, in 2008, and the HDR degree (by research), in 2017. In 2009, he became an Associate Professor with the Laboratoire d'Ingénierie des Systèmes de Versailles (LISV), University of Versailles. His research interests include sensors and interactions, especially in the field of micro-robotics.